

## Work distribution in manipulated single biomolecules

This article has been downloaded from IOPscience. Please scroll down to see the full text article.

2009 Phys. Biol. 6 025011

(<http://iopscience.iop.org/1478-3975/6/2/025011>)

The Table of Contents and more related content is available

Download details:

IP Address: 130.225.29.254

The article was downloaded on 01/07/2009 at 14:31

Please note that terms and conditions apply.

# Work distribution in manipulated single biomolecules

A Imparato<sup>1</sup> and L Peliti<sup>2,3</sup>

<sup>1</sup> Department of Physics and Astronomy, University of Aarhus, Ny Munkegade, Building 1520, DK-8000 Aarhus C, Denmark

<sup>2</sup> Kavli Institute for Theoretical Physics, University of California, Santa Barbara, CA 93106-4030, USA

<sup>3</sup> Dipartimento di Scienze Fisiche and Unità INFN, Università 'Federico II', Complesso Monte S. Angelo, I-80126 Napoli, Italy

E-mail: [imparato@phys.au.dk](mailto:imparato@phys.au.dk) and [peliti@na.infn.it](mailto:peliti@na.infn.it)

Received 14 November 2008

Accepted for publication 13 January 2009

Published 1 July 2009

Online at [stacks.iop.org/PhysBio/6/025011](http://stacks.iop.org/PhysBio/6/025011)

## Abstract

We consider the relation between the microscopic and effective descriptions of the unfolding experiment on a model polypeptide. We evaluate the probability distribution function of the work performed by Monte Carlo simulations and compare it with that obtained by evaluating the work distribution generating function on an effective Brownian motion model tailored to reproduce exactly the equilibrium properties. The agreement is satisfactory for fast protocols, but deteriorates for slower ones, hinting at the existence of processes on several time scales even in such a simple system.

## 1. Introduction

By means of atomic force microscopes and optical tweezers, several experimental groups have been able to control very precisely the force applied to proteins and nucleic acids. The observation of the unfolding behavior of these molecules under mechanical stress represents a powerful tool to recover structural properties of proteins and nucleic acids [1–9].

Furthermore, in the case of small biomolecules, unfolding experiments represent an excellent test bed for a class of recently derived results, which go under the name of *fluctuation relations* [11–13]. These relations connect the energy exchanged by thermodynamical systems with their environment to their equilibrium properties, and therefore represent an intriguing bridge between equilibrium and nonequilibrium. The case of small biomolecules under external force is interesting in itself, since the fluctuations of the energy exchanged by these systems are of the order of their average thermal energy, and they are therefore an example of microscopic out-of-equilibrium systems, with very large thermal fluctuations, whose study is one of the current topical problems in statistical mechanics [14].

As a force is applied to a biomolecule, and it progressively unfolds, the external pulling device performs thermodynamical work on it. By sampling this quantity over many repetitions of the unfolding experiments, and taking

advantage of suitable fluctuation relations [11–13], it has been possible to estimate experimentally the free-energy difference between the folded and the unfolded states of a simple RNA hairpin [10] and the free-energy landscape of some proteins as a function of the molecular elongation [15, 16]. Convergence in such an estimate is dominated by the so-called outliers, i.e. rare values of the work that are much smaller than the average. The interest in the study of distribution functions of work performed on biomolecules during unzipping experiments and in particular of the distribution tails is due to the need to estimate the frequency of the rare events that ensure validity of the fluctuation relations.

The evaluation of the work probability distribution function (PDF) for a manipulated system requires in principle the solution of an evolution equation of complexity equivalent to the equation for the microscopic dynamics. Since this equation involves a large number of degrees of freedom even for comparatively small systems such as a polypeptide, it is customary to describe its dynamics by a small set of collective coordinates undergoing a Brownian diffusion process [13, 17–20]. It is worth noting that in their works, Hummer and Szabo [20] showed that if the molecular unfolding is described as a one-dimensional diffusion process along a structured energy potential, the force-induced rupture rate exhibits behavior which is much more complex than the widely used approach based on Bell's formula. Here we investigate

the relation between the two levels of description on a simple model of a polypeptide unfolding experiment, and differently from [20], we focus on the description of the work distribution rather than on the description of the unfolding rate.

## 2. The work distribution

Let us consider a system whose microscopic state is identified by the variable  $x$ , where  $x$  can also indicate a collection of microscopic coordinates, e.g. the positions and momenta of the particles which make up the system. We shall assume that the system evolves according to a general dynamic process, parametrized by a parameter  $\mu$ , which can be manipulated according to a fixed protocol  $\mu(t)$ . The evolution can be deterministic or stochastic, but we shall assume that, for any given value of  $\mu$ , there is a well-defined equilibrium distribution that can be represented in the Boltzmann–Gibbs form:

$$P_{\mu}^{\text{eq}}(x) = \frac{e^{-\beta H(x, \mu)}}{Z_{\mu}}, \quad (1)$$

a relation which defines the Hamiltonian  $H(x, \mu)$  and the partition function  $Z_{\mu} = \int dx e^{-\beta H(x, \mu)}$ . Here  $\beta = 1/k_B T$ , where  $T$  is the absolute temperature and  $k_B$  is Boltzmann's constant. Thus,  $H(x, \mu)$  depends explicitly on the time only via  $\mu(t)$ . The PDF  $P(x, t)$  of the microscopic state  $x$  evolves according to the Liouville-like partial differential equation:

$$\partial_t P(x, t) = \mathcal{L}_{\mu} p(x, t), \quad (2)$$

where  $\mathcal{L}_{\mu}$  is a linear differential operator, compatible with the equilibrium distribution of the system for any fixed value of  $\mu$ :  $\mathcal{L}_{\mu} P_{\mu}^{\text{eq}} = 0, \forall \mu$ .

The external manipulation of the system via  $\mu$  leads to an energy exchange with the environment. According to the usual conventions in statistical mechanics (see, e.g., [21]), the fluctuating work  $W$  performed on the system, given the manipulation protocol  $\mu(t)$  and the microscopic trajectory  $x(t)$ , is given by

$$W = \int_0^t dt' \dot{\mu}(t') \partial_{\mu} H(x, \mu)|_{x(t'), \mu(t')}. \quad (3)$$

Under these hypotheses, the time evolution of the joint PDF  $\phi(x, W, t)$  of the microscopic state  $x$  and the total work  $W$  performed on the system is governed by the partial differential equation [17, 18]

$$\begin{aligned} \partial_t \phi(x, W, t) &= \mathcal{L}_{\mu} \phi(x, W, t) \\ &\quad - \dot{\mu}(t) \partial_{\mu} H(x, \mu)|_{\mu(t)} \partial_W \phi(x, W, t). \end{aligned} \quad (4)$$

In order to simplify the analysis, one evaluates the generating function  $\psi(x, \lambda, t)$  of the distribution of  $W$ , defined by

$$\psi(x, \lambda, t) = \int dW e^{i\lambda W} \phi(x, W, t), \quad (5)$$

so that equation (4) becomes

$$\partial_t \psi(x, \lambda, t) = \mathcal{L}_{\mu} \psi(x, \lambda, t) + i\lambda \partial_t H \psi(x, \lambda, t). \quad (6)$$

This equation can be solved explicitly if the system is characterized by discrete states: in [22], e.g., an RNA hairpin was modeled as a three-state system and the PDF of the work,

done on the molecule by an external mechanical force, was evaluated numerically.

One can evaluate the solution of equations (5) and (6) for real  $\lambda$ , starting from the initial condition  $\psi(x, \lambda, 0) = P^{\text{eq}}(0), \forall \lambda$ . Thus, since  $\phi(x, W, t)$  is real, we have  $\psi(x, -\lambda, t) = \psi^*(x, \lambda, t)$  and we can restrict ourselves to the half-line  $\lambda \geq 0$ . Then one can separate equation (6) into two equations, one for the real part  $\psi_R$  and one for the imaginary part  $\psi_I$  of  $\psi$ , obtaining

$$\partial_t \psi_R(x, \lambda, t) = \mathcal{L}_{\mu} \psi_R(x, \lambda, t) - \lambda \partial_t H \psi_I(x, \lambda, t), \quad (7)$$

$$\partial_t \psi_I(x, \lambda, t) = \mathcal{L}_{\mu} \psi_I(x, \lambda, t) + \lambda \partial_t H \psi_R(x, \lambda, t). \quad (8)$$

Once the function  $\psi(x, \lambda, t)$  has been obtained, the joint PDF  $\phi(x, W, t)$  is given by the inverse Fourier transform of  $\psi(x, \lambda, t)$ . The unconstrained work PDF can then be evaluated from the relation  $\Phi(W, t) = \int dx \phi(x, W, t)$ .

An important special case is obtained when one considers a system described by few degrees of freedom, which is in contact with a large heat reservoir. In this case, it is often warranted to assume that the microscopic state  $x$  performs Brownian motion [13, 17–20], and thus the operator  $\mathcal{L}_{\mu}$  has the form of a Fokker–Planck (FP) differential operator:

$$\mathcal{L}_{\mu} \cdot = \Gamma \frac{\partial}{\partial x} \left[ \partial_x H(x, \mu) \cdot + k_B T \frac{\partial}{\partial x} \cdot \right], \quad (9)$$

where we take into account the Einstein relation between the diffusion and the kinetic (mobility) coefficients  $D = \Gamma k_B T$ .

## 3. Collective coordinates

In an unfolding experiment, where a mechanical force is applied to one or both of the free ends of a biopolymer, the work can be sampled by monitoring the extension of the molecules at different times [10, 15, 16]. In this situation, we face the following problem. Equations (2), (4) and (6) describe the dynamics of a system at a very detailed, microscopic level. On the other hand, the behavior of the system is accessed only via the measurement of a few, and most often only one, observables, such as the elongation. Moreover, the microscopic ‘Liouville’ operator is not generally known with sufficient confidence. In any case, the explicit solution of the evolution equations becomes unfeasible as soon as more than a few degrees of freedom have to be considered.

Thus, one considers descriptions of the system through some experimentally accessible collective coordinates. In the case of biopolymers, one typically chooses the end-to-end length  $L$ . Its equilibrium distribution is determined by the effective free energy, defined by

$$F(L, \mu) = -\beta^{-1} \ln \int dx \delta(L(x) - L) e^{-\beta H(x, \mu)}, \quad (10)$$

which plays the role of an effective Hamiltonian. The dependence of this free energy on  $L$  is the target of several experimental studies, performed by using a suitable fluctuation relation [15, 16].

It should be possible in principle to obtain the evolution for the collective coordinate PDF, and thus the work distribution, by projecting the microscopic ‘Liouville’ equations on the

space spanned by the collective coordinates [23]. However, one would then in general obtain complicated non-Markovian evolution equations, whose parameters will depend on unknown details of the underlying microscopic dynamics. In other words, even if equations (2)–(6) were exact, it would be hard to derive the explicit equations governing the time evolution of the PDF  $P(L, t)$  and the joint PDF  $\phi(L, W, t)$ .

Thus, in the present work, we make the following ansatz: we assume that the coordinate  $L$  performs Brownian motion in an effective potential, which is given by the free-energy landscape (10). This implies that the evolution operator  $\mathcal{L}_\mu$  for the coordinate  $L$  is an FP operator of the form of equation (9), where  $x$  has to be replaced by  $L$  and  $H(x, \mu)$  has to be replaced by  $F(L, \mu)$ , as given by equation (10). This is a bold summary of the underlying microscopic process. In the resulting model, the form of the evolution equation is constrained, but the value of the kinetic coefficient  $\Gamma$  is still free. We shall take advantage of this degree of freedom and check whether it allows us to describe the behavior of the work PDF with sufficient fidelity.

#### 4. Lattice model of proteins

In the present section we consider a lattice model for proteins under mechanical load, which, in spite of its simplicity, is able to reproduce in great detail the outcome of experiments performed on real proteins [24–26]. In this model, the state of a  $N + 1$  amino acid protein is defined by the set of discrete variables  $\{m_k\}$ ,  $k = 1, \dots, N$ . These binary variables take the value  $m_k = 0$  ( $m_k = 1$ ), if the peptide bond is in the non-native (native) configuration. Then the effective Hamiltonian reads

$$H_{\text{eff}}(\{m_k\}, L, f) = \sum_{i=1}^{N-1} \sum_{j=i+1}^N \epsilon_{ij} \Delta_{ij} \prod_{k=i}^j m_k - f \cdot L(\{m_k\}, \{\sigma_{ij}\}), \quad (11)$$

where

$$L(\{m_k\}, \{\sigma_{ij}\}) = \sum_{0 \leq i < j \leq N+1} l_{ij} \sigma_{ij} S_{ij}(m) \quad (12)$$

is the end-to-end distance in the configuration  $x = (\{m_k\}, \{\sigma_{ij}\})$ , projected on the direction of the applied force, as shown in figure 1. In this Hamiltonian the quantity  $\epsilon_{ij} \leq 0$  represents the interaction energy between the residues  $i$  and  $j + 1$ ,  $l_{ij}$  is the length of the native strand of peptide bonds between residues  $i$  and  $j$ , or the length of the single non-native bond  $i, i + 1$ , and the binary variable  $\sigma_{ij}$  is equal to 1 if the strand is parallel and to  $-1$  if it is antiparallel to the applied force. The quantity  $S_{ij}(m)$  is equal to 1 if the polypeptide strand starting at  $i$  and ending at  $j$  is all in the native state, and is flanked by bonds in the non-native state, and vanishes otherwise, as explained in [24, 25]. For a given protein, the parameters  $\epsilon_{ij}$  and  $l_{ij}$  are obtained by analyzing the protein native structure, as given in the protein data bank (PDB).

Here, we consider in particular the polypeptide PIN1 (PDB code 1I6C) which is made up of 39 amino acids, at a reduced temperature  $\tilde{T} = 6$  (cf [25] for a detailed discussion on the temperature and force scales).

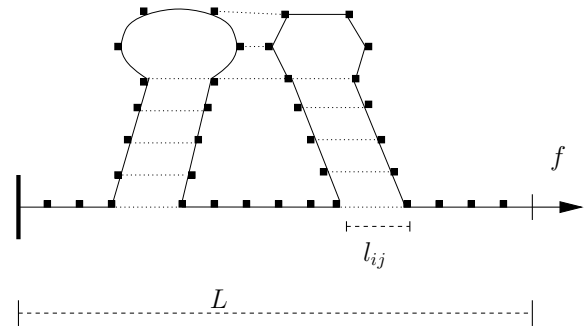


**Figure 1.** Image of the model protein, with a force applied to one of the free ends. Dots denote amino acids and dashed lines denote contacts.

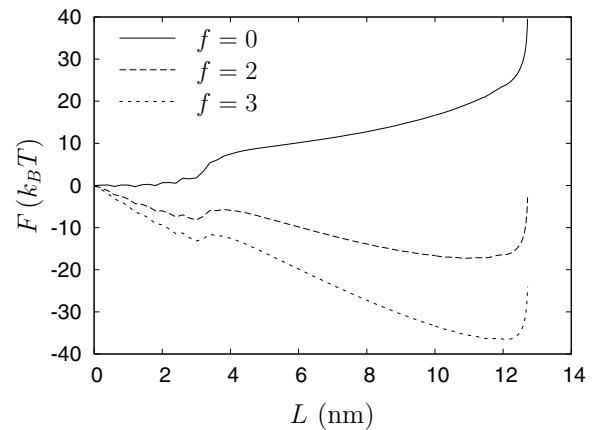


**Figure 2.** Free-energy landscape  $F(L, f)$  for the model PIN1 polypeptide, for different values of the external force. The force is expressed in reduced units; see [25].

The unfolding experiments are simulated using the Monte Carlo Metropolis algorithm with the Hamiltonian (11), where the external force varies linearly with time  $f = r \cdot t$ . For each unfolding trajectory, the system is prepared in equilibrium with vanishing force, and then at  $t = 0$ , the force starts increasing with rate  $r$ . For practical purposes, we define the force rate as  $r = f_{\text{max}}/t_{\text{max}}$ , keeping  $f_{\text{max}} = 10$  constant and varying  $t_{\text{max}}$ . We have simulated 10 000 unfoldings for each value of the rate  $r$ . We have then sampled the work  $W = \int_0^{t_{\text{max}}} \partial_t H_{\text{eff}}(\{m_k\}, \{\sigma_{ij}\}, f(t)) dt$  performed on the molecule and evaluated the work histograms.

For the model protein considered here, the free-energy landscape  $F_0(L)$ , as defined by

$$F_0(L) = -k_B T \ln \left\{ \sum_x \exp[-\beta H_{\text{eff}}(x, f=0)] \delta(L(x) - L) \right\}, \quad (13)$$

can be exactly calculated [24, 25], and the time-dependent landscape therefore reads as  $F(L, f(t)) = F_0(L) - f(t)L$ . In equation (13),  $x$  represents the microscopic state of the model, i.e. the collection of the variables  $\{m_k\}$  representing the state of the bonds and of the variables  $\{\sigma_{ij}\}$  representing the orientation of the strands with respect to the reference direction.

The free-energy landscape  $F(L, f)$  of this polypeptide is plotted in figure 2, for different values of the external

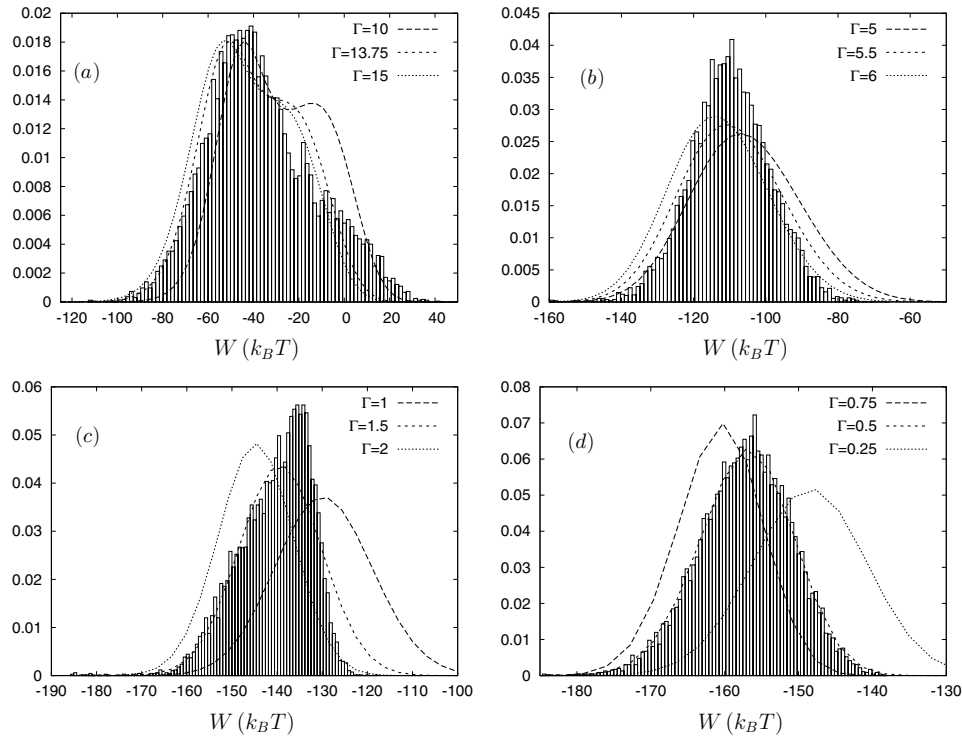


**Figure 3.** Work PDF for the model protein discussed in the text, for different values of the force rate  $r$ :  $r = 1$  (a),  $r = 0.1$  (b),  $r = 0.01$  (c),  $r = 0.001$  (d). The value of  $\Gamma$ , shown in the legend of each figure, corresponds to the value used to numerically solve equation (6).

force. Inspection of this figure indicates that at a vanishing external force, the potential is almost flat for  $L \leq 3$  nm, while for larger values of the force a minimum appears at  $L^* \simeq 12.6$  nm, whose position is practically independent of  $f$ , indicating that  $L^*$  represents the length of the fully stretched molecule [25]. As discussed in section 3, we will take this energy landscape as effective potential in the differential operator (9).

In figure 3 we show the histograms of the work PDF, as obtained by the simulations discussed above, for four different values of the manipulation rate  $r = f_{\max}/t_{\max}$ . In the same figure, we plot the probability distribution function as obtained by solving a discretized version of equations (4)–(6).

In this approach the equations take the form of a master equation, in which the states are identified by an integer  $i$ , where  $L_i$  is the polymer length measured in units  $\Delta L = L_{\max}/N$ , where  $L_{\max}$  is the maximum length that can be obtained in the lattice model and  $N = 126$ . Positive and negative values of  $L$  are considered. The transition rates  $W_{i \rightarrow i \pm 1}$  are defined to match those of a Metropolis process with an attempt frequency equal to  $\Gamma$ :

$$W_{i \rightarrow j(i \pm 1)}(t) = \Gamma \times \begin{cases} 1, & \text{if } F(L_j, f(t)) \leq F(L_i, f(t)); \\ e^{-\beta(F(L_j, f(t)) - F(L_i, f(t)))}, & \text{otherwise.} \end{cases} \quad (14)$$

The resulting equations can then be solved, by a classic Runge–Kutta method, when a definite value is assigned to the kinetic parameter  $\Gamma$ . One then evaluates the unconstrained generating functions  $\Psi_{R,I}(\lambda, t_{\max}) = \int dL \psi_{R,I}(L, \lambda, t_{\max})$ . These functions are plotted in figure 4, for  $\Gamma = 13.75$ ,

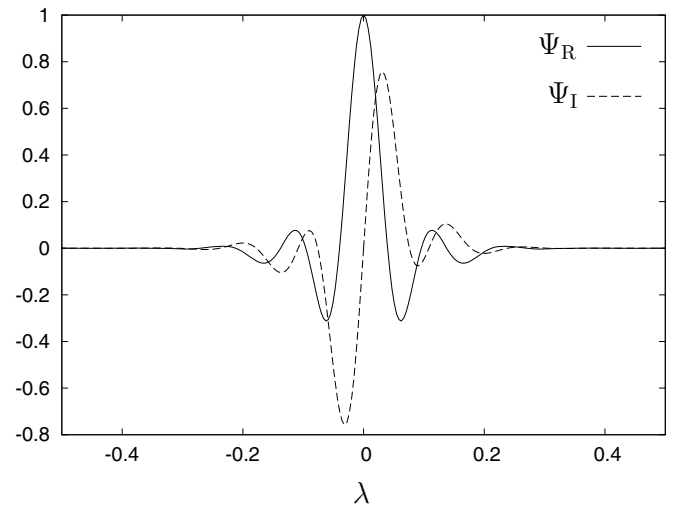


**Figure 4.** Real and imaginary parts of the unconstrained generating function  $\Psi(\lambda, t_{\max}) = \Psi_R(\lambda, t_{\max}) + i\Psi_I(\lambda, t_{\max})$  versus  $\lambda$ , as obtained from the numerical solutions of equations (7) and (8), with  $\Gamma = 13.75$ , and  $r = 1$  ( $t_{\max} = 10$ ).

and  $r = 1$  ( $t_{\max} = 10$ ). As discussed in section 2, the unconstrained work PDF  $\Phi(W, t_{\max})$  is finally obtained by inverting equation (5).

For each value of  $r$ , we consider different values of the kinetic coefficient  $\Gamma$  and choose the value which most closely reproduces the simulated histograms. Indeed, even if the microscopic process goes on with a well-defined characteristic attempt frequency, this is not the case for the effective process described by the FP equation. In order for  $x$  to change, the

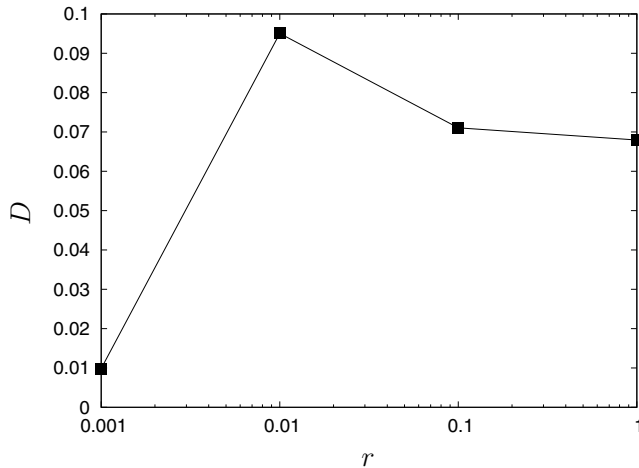


**Figure 5.** Kolmogorov–Smirnov distance  $D$  between the work distributions as obtained by simulations and by equations (4)–(6), as a function of the loading rate  $r$ .

microscopic variables  $\{m_k, \sigma_{ij}\}$  must change. Their rate of change will depend on an Arrhenius factor depending on the actual energy difference due to the change of the particular value one is looking at. This factor will depend on the instantaneous value of the applied force, as well as on the overall state of the chain, and will not be a function only of  $L$ . Nevertheless, we find that it is possible to identify a value of  $\Gamma$  which yields a reasonably good agreement for the faster protocols ( $r = 1$ ). This value decreases as the manipulation speed decreases, showing that in the slower manipulations there is a larger frequency of microscopic processes that does not show up in changes of  $L$ . For slower protocols ( $r = 0.1, 0.01$ ), while one can match the mean value of the calculated work PDF that was obtained with simulations, the shape of the calculated distribution differs from the histograms. Apparently the intrinsic rate of the microscopic processes in these protocols cannot be represented by a single attempt frequency, while it can for the faster protocols, which are dominated by simple ‘snatching off’ of native regions. For the slowest manipulations ( $r = 0.001$ ), the work distribution becomes Gaussian. In this case, the Jarzynski identity [11, 12] implies that its average  $W_0$ , its variance  $\sigma_W^2$  and the free-energy change  $\Delta F$  must be related by

$$W_0 = \Delta F + \frac{\beta \sigma_W^2}{2}. \quad (15)$$

Thus it is possible to recover the distribution by fitting the single parameter  $\Gamma$ , as we can see from the curves for  $r = 0.001$ .

In order to compare quantitatively the work PDFs as obtained by simulations and by solutions of equations (4)–(6), for each value of  $r$  we exploit the Kolmogorov–Smirnov test [27]. Thus, one evaluates the maximal distance  $D$  between the cumulative distributions of the two work PDFs:

$$D = \sup_x |\chi^{\text{exp}}(W) - \chi^{\text{theo}}(W)|, \quad (16)$$

where  $\chi^\alpha(W) = \int_{-\infty}^W dW \Phi^\alpha(W)$ ,  $\alpha = \text{exp/theo}$ , and where  $\Phi^{\text{exp}}(W)$  is the histogram as obtained by simulations and  $\Phi^{\text{theo}}(W)$  is the expected distribution, obtained with the

procedure described in section 2. The quantity  $D$  is plotted in figure 5 as a function of  $r$ . Inspection of this figure suggests that the smallest values of  $D$  are obtained for  $r = 1$  and  $r = 0.0001$ , as indicated by a qualitative analysis of figure 3.

## 5. Discussion

In this work, we have investigated a simple example of the relation between the work PDF obtained for the same system via its microscopic dynamics and an effective Brownian dynamics. We found that the Brownian dynamics works reasonably well for the faster protocols, but is off the mark for slower ones, hinting at the existence of several dynamical time scales in the relaxation of a moderately complex manipulated system. Thus, particular care has to be taken when comparing experimental outcomes with the results of numerical simulations, when the unfolding of a biopolymer is modeled as a biased one-dimensional Brownian process.

## Acknowledgments

LP completed this research while visiting the Kavli Institute for Theoretical Physics within the program *FLUCTUATE08*. This research was supported in part by the National Science Foundation under grant no. PHY05-51164. AI is grateful to A Pelizzola and M Zamparo for introducing him to the lattice model discussed in section 4.

## References

- [1] Kellermayer M S, Smith S B, Granzier H L and Bustamante C 1997 Folding-unfolding transitions in single titin molecules characterized with laser tweezers *Science* **276** 1112
- [2] Carrion-Vasquez M *et al* 1999 Mechanical and chemical unfolding of a single protein: a comparison *Proc. Natl Acad. Sci.* **96** 3694
- [3] Carrion-Vasquez M *et al* 2003 The mechanical stability of ubiquitin is linkage dependent *Nat. Struct. Biol.* **10** 738
- [4] Dietz H and Rief M 2004 Exploring the energy landscape of GFP by single-molecule mechanical experiments *Proc. Natl Acad. Sci.* **101** 16192
- [5] Dietz H, Berkemeier F, Bertz M and Rief M 2006 Anisotropic deformation response of single protein molecules *Proc. Natl Acad. Sci.* **103** 12724
- [6] Oberhauser A F, Hansma P K, Carrion-Vasquez M and Fernandez J M 2001 Stepwise unfolding of titin under force-clamp atomic force microscopy *Proc. Natl Acad. Sci.* **98** 468
- [7] Li H *et al* 2000 Atomic force microscopy reveals the mechanical design of a modular protein *Proc. Natl Acad. Sci.* **97** 6527
- [8] Fernandez J M and Li H 2004 Force-clamp spectroscopy monitors the folding trajectory of a single protein *Science* **303** 1674
- [9] Schlierf M, Li H and Fernandez J M 2004 The unfolding kinetics of ubiquitin captured with single-molecule force-clamp techniques *Proc. Natl Acad. Sci.* **101** 7299
- [10] Danilowicz C *et al* 2003 DNA unzipped under a constant force exhibits multiple metastable intermediates *Proc. Natl Acad. Sci.* **100** 1694
- [11] Liphardt J *et al* 2001 Reversible unfolding of single RNA molecules by mechanical force *Science* **292** 733
- [12] Onoa B *et al* 2003 Identifying kinetic barriers to mechanical unfolding of the *T. thermophila* ribozyme *Science* **299** 1892

- [10] Liphardt J, Dumont S, Smith S, Tinoco I and Bustamante C 2002 Equilibrium information from nonequilibrium measurements in an experimental test of Jarzynski's equality *Science* **296** 1832  
Collin D, Ritort F, Jarzynski C, Smith S B, Tinoco Jr I and Bustamante C 2005 Verification of the Crooks fluctuation theorem and recovery of RNA folding free energies *Nature* **437** 231
- [11] Jarzynski C 1997 Nonequilibrium equality for free energy differences *Phys. Rev. Lett.* **78** 2690  
Jarzynski C 1997 Equilibrium free-energy differences from nonequilibrium measurements: a master-equation approach *Phys. Rev. E* **56** 5018
- [12] Crooks G E 1998 Nonequilibrium measurements of free energy differences for microscopically reversible Markovian systems *J. Stat. Phys.* **90** 1481  
Crooks G E 1999 Entropy production fluctuation theorem and the nonequilibrium work relation for free energy differences *Phys. Rev. E* **60** 2721
- [13] Hummer G and Szabo A 2001 Free energy reconstruction from nonequilibrium single-molecule pulling experiments *Proc. Natl Acad. Sci.* **98** 3658
- [14] Ritort F 2008 Nonequilibrium fluctuations in small systems: from physics to biology *Adv. Chem. Phys.* **137** 31
- [15] Harris N C, Song Y and Kiang C-H 2007 Experimental free energy surface reconstruction from single-molecule force spectroscopy using Jarzynski's equality *Phys. Rev. Lett.* **99** 068101
- [16] Imparato A, Sbrana F and Vassalli M 2008 Reconstructing the free-energy landscape of a polyprotein by single-molecule experiments *Europhys. Lett.* **82** 58006
- [17] Imparato A and Peliti L 2005 Work distribution and path integrals in general mean-field systems *Europhys. Lett.* **70** 740
- [18] Imparato A and Peliti L 2005 Work-probability distribution in systems driven out of equilibrium *Phys. Rev. E* **72** 046114
- [19] Braun O, Hanke A and Seifert U 2004 Probing molecular free energy landscapes by periodic loading *Phys. Rev. Lett.* **93** 158105
- [20] Hummer G and Szabo A 2003 Kinetics from nonequilibrium single-molecule pulling experiments *Biophys. J.* **85** 5  
Dudko O K, Hummer G and Szabo A 2006 Intrinsic rates and activation free energies from single-molecule pulling experiments *Phys. Rev. Lett.* **96** 108101
- [21] Peliti L 2008 On the work-Hamiltonian connection in manipulated systems *J. Stat. Mech.* **P05002**
- [22] Imparato A and Peliti L 2005 Work probability distribution in single-molecule experiments *Europhys. Lett.* **69** 643
- [23] Mori H 1965 Transport, collective motion, and Brownian motion *Prog. Theor. Phys.* **33** 423
- [24] Imparato A, Pelizzola A and Zamparo M 2007 Ising-like model for protein mechanical unfolding *Phys. Rev. Lett.* **98** 148102
- [25] Imparato A, Pelizzola A and Zamparo M 2007 Protein mechanical unfolding: a model with binary variables *J. Chem. Phys.* **127** 145105
- [26] Imparato A and Pelizzola A 2008 Mechanical unfolding and refolding pathways of ubiquitin *Phys. Rev. Lett.* **100** 158104
- [27] Eadie W T, Drijard D, James F E, Roos M and Sadoulet B 1971 *Statistical Methods in Experimental Physics* (Amsterdam: North-Holland)